POLITECNICO DI TORINO
Repository ISTITUZIONALE

Investigation of Programmability in MZI-based Clements Meshes for Photonic Logical Operations

Original
Investigation of Programmability in MZI-based Clements Meshes for Photonic Logical Operations / Ma, T., Marchisio, A., Curri, V., Bardella, P., Carena, A.. - (2026), pp. 1-4. (International Conference on Transparent Optical Networks (ICTON) Prague (Cze) 12-16 July 2026) [10.1109/icton71309.2026.11705332].

Availability:
This version is available at: 11583/3016325 since: 2026-10-05T10:30:47Z

Publisher:
IEEE

Published
DOI:10.1109/icton71309.2026.11705332

Terms of use:

This article is made available under terms and conditions as specified in the corresponding bibliographic description in the repository

Publisher copyright
IEEE postprint/Author's Accepted Manuscript

©2026 IEEE. Personal use of this material is permitted. Permission from IEEE must be obtained for all other uses, in any current or future media, including reprinting/republishing this material for advertising or promotional purposes, creating new collecting works, for resale or lists, or reuse of any copyrighted component of this work in other works.

(Article begins on next page)

20 October 2026

Investigation of Programmability in MZI-based Clements Meshes for Photonic Logical Operations

Teng Ma
Politecnico di Torino
Torino, Italy
teng.ma@polito.it

Andrea Marchisio
Politecnico di Torino
Torino, Italy
andrea_marchisio@polito.it

Vittorio Curri
Politecnico di Torino
Torino, Italy
vittorio.curri@polito.it

Paolo Bardella
Politecnico di Torino
Torino, Italy
paolo.bardella@polito.it

Andrea Carena
Politecnico di Torino
Torino, Italy
andrea.carena@polito.it

***Abstract*—In this work, we analyze the impact of the Coupling Layer (CL) topology on the operation of a 3×3 mesh of Mach-Zehnder Interferometers (MZIs) in Clements configuration, when employed to implement user-defined logical operations. By adopting a Genetic Algorithm (GA)-based optimization method, we determine optimal phase shifts for each MZI in the Clements mesh to achieve a specific logical operation, given a fixed CL topology. We investigate device programmability based on numerical simulation using both the Extinction Ratio (ER) and the Threshold Ratio (TR) metrics, demonstrating that some CL topologies can support more than 80% of all possible truth tables with an ER greater than 3 dB. We analyze in detail the device programmability based on a case study of a specific CL topology with good ER performance, finding that it can implement at least 16 Boolean functions with an ER greater than 5 dB. These results provide insights for photonic chip design and testing.**

***Index Terms*—Photonic Integrated Circuits, Programmability, Mach-Zehnder Interferometer, Coupling Layer, Clements mesh.**

I. Introduction

By employing light instead of electrical signals to perform logical operations, photonic logic gates offer ultra-fast signal processing with better energy-efficiency compared to their traditional electronic counterparts, serving as a promising technology for a wide range of applications, such as Artificial Intelligence (AI), high-performance computing, and telecommunication networks [1], [2]. Photonic logic gates are typically implemented with devices that rely on optical nonlinearities such as Cross-Gain Modulation (XGM), Cross-Phase Modulation (XPM), and Four-Wave Mixing (FWM), and that are modulated in optical power. However, these implementations suffer from several drawbacks such as high power consumption, limited scalability, susceptibility to noise, etc [3]–[5]. For this reason, an all-optical approach that does not depend on optical nonlinearities for programmable logic gates could be beneficial to overcome these issues.

In the last decade, Optical Inference Units (OIUs) based on the Clements architecture have been adopted in Machine Learning (ML) applications to implement parallel optical matrix multiplication [6]. Recent research demonstrates that an OIU can enable several linear optical operations if the phase shift parameters of each Mach Zehnder Interferometer (MZI) are optimized and if a Coupling Layer (CL) is introduced to combine the matrix-vector multiplication results of OIU [7].

In this work, we study the impact of different CL topologies on the general programmability of a 3×3 Clements MZI mesh, taking all possible output combinations into consideration. Based on the Mean Squared Error (MSE) measure that quantifies the average squared difference between the output power values and the corresponding values specified in the truth table, we obtained the optimal phase shift parameters for each MZI in the Clements mesh, for every possible logical operation in each CL topology. By using the method reported in [8], we evaluated the programmability of the proposed scheme under different CL topologies, demonstrating the capability of some CL topologies to implement more than 80% of all possible truth tables with good output signal quality. We also investigated in detail a practical case study by selecting a specific CL topology, finding that 16 Boolean functions can be implemented with high reliability.

II. Reference Device and Model

As shown in Fig. 1, the proposed scheme includes the 3×3 Clements MZI mesh, the CL based on optical splitters/couplers, and two output ports (P and Q). The A and B optical digital signals are fed to Input Port 1 and Input Port 2, respectively. A constant input value is applied to Input Port 3 of the Clements mesh. The O_1, O_2, and O_3 represent the

T.M. Ph.D. scholarship is funded by the Chinese Scholarship Council (CSC) under File No. 202507820037. A.M. Ph.D. scholarship is funded by the European Union Next-GenerationEU and by the Italian National Recovery and Resilience Plan (PNRR) through the Italian Ministry of University and Research (MUR) under grant D.M.352/2022.

979-8-3195-4420-9/26/$31.00 ©2026 IEEE

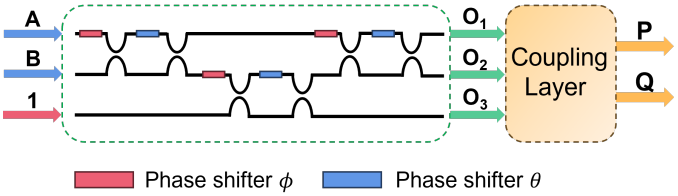

Fig. 1. Proposed scheme for the device implementing programmable logical operations. Blue and red rectangles highlight the positioning of phase shifters in each MZI.

Output Ports of the Clements mesh. The CL linearly sums the matrix multiplication results from the Clements mesh and exports them to the P and Q device output ports.

The input logic states are encoded in the amplitude of the optical pulses. The logical relation in the proposed scheme is expressed as follows [7]:

$$Y = XUC \tag{1}$$

where:

- X represents a 4×3 binary matrix considering all input combinations of A and B;
- Y denotes a 4×2 binary matrix where each row represents a corresponding output state;
- C is a 3×2 binary matrix with each column representing the topological CL connection between an Output Port of the Clements mesh (O_1, O_2 and O_3) and the output ports of the proposed scheme (P and Q): each output port of the proposed scheme can be optically connected to either one, two, or three Output Ports of the Clements mesh;
- U is a 3×3 unitary matrix that is obtained through the decomposition method presented in [9].

Each MZI consists of two lossless 50:50 directional couplers and two phase shifters parameterized by (ϕ, θ) and applies the following unitary transformation:

$$M = \begin{bmatrix} e^{j\phi}\cos\theta & -\sin\theta \\ e^{j\phi}\sin\theta & \cos\theta \end{bmatrix} \tag{2}$$

where θ lies in the interval $[0, \pi/2]$, and ϕ lies in the interval $[0, 2\pi]$.

Taking all possible cases into consideration, there are $2^6 = 64$ possible C matrices. However, some matrices cannot generate practical CL topologies. Given that our programmability investigation takes into account the optical power in both P and Q ports, we exclude those CL topologies that only connect to a single port (either P or Q) and the CL topology with null matrix C, reducing the number of valid CL topologies to 49.

Moreover, due to the fact that the truth values in P and Q ports are different in the majority of all possible 256 logical operations, we also abandon the CL topologies where any connected Output Port of Clements mesh always has connection to both P and Q ports, thus setting the number of valid considered CL topologies to 42.

Fig. 2 illustrates some examples of topological connections of the CL, represented by a specific matrix C. Assuming that

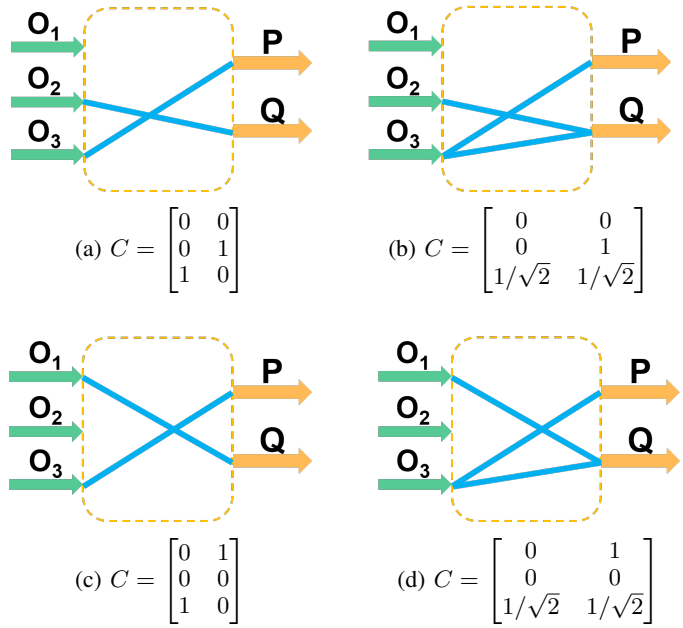

Fig. 2. Examples of topological connections of the Coupling Layer represented by a specific matrix C.

the optical waveguides and the optical crossings are lossless, we do not take loss factor into account when assigning values to the matrix C. We assign value 1 to the element in the matrix C representing an Output Port of the Clements mesh that has connection to only one single output port (either P or Q) of the proposed scheme, while the value $1/\sqrt{2}$ is assigned to the rows of the matrix C representing an Output Port of Clements mesh that has connections to both P and Q ports to account for power splitting.

III. Programmability Investigation

Given the complexity and nonlinearity when deriving the analytical solution in Eq. (1), we reformulate the problem as an optimization task to find the best numerical solution that meets the transformation mapping from X to Y. We have implemented the optimization using MATLAB on an Intel® i9 12th generation workstation. We have developed our optimization method based on Genetic Algorithm (GA) [10] to find the global optimal solution of phase shift parameters in the input domain of Eq. (2), as well as leveraging the `fmincon` function in the MATLAB Optimization Toolbox to prevent premature convergence of GA.

For the GA optimizer, the Population Size parameter is set to 10^4, the Maximum Number of Generations parameter to 10^3, and the Crossover Rate parameter to 0.8. In each CL topology, for every possible truth table, we determined the optimal values of all phase shifters in the Clements mesh to minimize the fitness function, namely the MSE, which is defined as follows:

$$f(\mathbf{\Psi}) = \frac{1}{8}\sum_{i=1}^{8}(P_i - Y_i)^2 \tag{3}$$

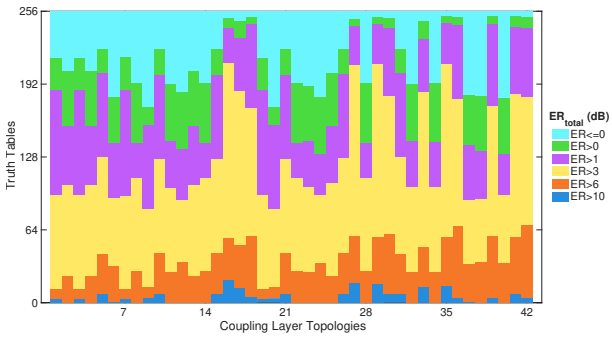

Fig. 3. Histogram of the programmability analysis.

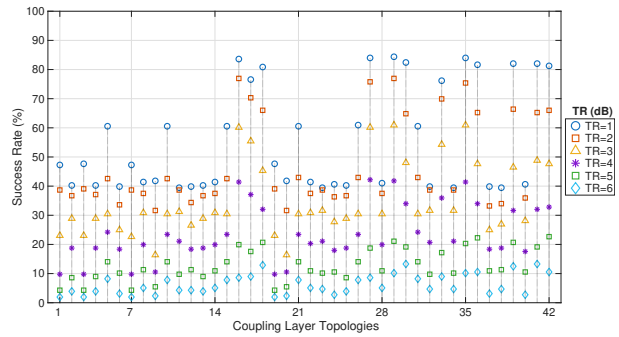

Fig. 4. Programmability evaluation under different TR.

where $\mathbf{\Psi}$ is the set of phases to be tuned at the phase shifters. P_i and Y_i represent the calculated output power and the truth value for the i-th bit in the specified truth table, respectively.

We evaluated the programmability of the proposed scheme to implement all possible 256 logical operations under all different practical CL topologies. The quality of output signals can be measured in terms of the total Extinction Ratio (ER) as follows:

$$\mathrm{ER}_{\mathrm{total}}(\mathrm{dB}) = 10\log_{10}\left(\frac{\min(P_1, Q_1)}{\max(P_0, Q_0)}\right) \tag{4}$$

where P_1 and Q_1 represent the power values of logical "1" cases at P and Q ports, respectively. P_0 and Q_0 represent the power values of logical "0" cases at P and Q ports, respectively.

In Fig. 3 we report the statistical distribution of the $\mathrm{ER}_{\mathrm{total}}$ parameter for all truth tables and for each CL topology through a histogram. We found that some CL topologies can reproduce more than 80% of the truth tables, guaranteeing an $\mathrm{ER}_{\mathrm{total}}$ greater than 3 dB.

To better understand the resilience of the proposed scheme to signal disturbances (optical noise, quantization noise, etc.), we carried out a further analysis. We set two different thresholds for logical "1" and "0" cases [8], which are defined as follows:

$$P_{th,k,1} = (1+c)\cdot P_{\mathrm{m},k} \tag{5}$$

$$P_{th,k,0} = (1-c)\cdot P_{\mathrm{m},k} \tag{6}$$

where $P_{\mathrm{m},k}$ is the median value of the power distribution for all truth tables at the k-th output port (k refers to P and Q output ports, respectively). The constant c is defined to distinguish the lower and upper thresholds; any power value falling between these two thresholds is discarded to prevent any issues related to power fluctuations. Based on these two thresholds, we obtain the logical values on both P and Q output ports and we compare the logical values with nominal truth tables.

In order to evaluate the effect of the threshold programmability constant, we defined the Threshold Ratio (TR), which is formulated as follows:

$$\mathrm{TR}(\mathrm{dB}) = 10\log_{10}\left(\frac{1+c}{1-c}\right). \tag{7}$$

Given a specific TR value, we calculate the corresponding constant c based on Eq. (7), then a logical operation is considered feasible if all 8 logical values, based on the two thresholds, match the truth values in the corresponding truth table.

Aiming to assess the capability of the proposed scheme to implement all possible 256 logical operations, we introduced the following success ratio definition:

$$\mathrm{SR}_{\%} = \frac{\text{Number of feasible logical operations}}{\text{Number of possible logical operations}} \times 100. \tag{8}$$

We finally evaluated the success ratio of programmability of the proposed scheme under different TR limits ranging from 1 to 6 dB with 1 dB step. In Fig. 4 we report the comprehensive analysis of $\mathrm{SR}_{\%}$ values for all CL topologies while varying the TR limit. It can be observed that different CL topology has very different success ratio of programmability. In general, $\mathrm{SR}_{\%}$ values decrease as the TR limit becomes more stringent. However, the overall trend of $\mathrm{SR}_{\%}$ values remains consistent under different TR limits and aligns with the trend of $\mathrm{ER}_{\mathrm{total}}$ values in Fig. 3. In specific instances, some CL topologies can realize over 80% of the truth tables under 1 dB TR limit while maintaining programmability on more than 70% of the truth tables under a less stringent 2 dB TR limit.

IV. Case Study: Boolean Logic with Fixed CL

We studied in detail a practical case based on the 16th CL topology out of the 42 CL topologies analyzed, which is one of the best CL topologies with good $\mathrm{ER}_{\mathrm{total}}$ performance in Fig. 3 and very high $\mathrm{SR}_{\%}$ values in Fig. 4. The topology of the CL for this specific selected C is shown in Fig. 5. The P port connects to the O_2 and O_3 ports of the Clements mesh, while the Q port connects to the O_1 and O_3 ports of the Clements mesh. Considering the power splitting in the O_3 port of the Clements mesh, the matrix C for this case is determined as

$$C = \begin{bmatrix} 0 & 1 \\ 1 & 0 \\ 1/\sqrt{2} & 1/\sqrt{2} \end{bmatrix}. \tag{9}$$

We tested the programmability of the case study to implement user-defined Boolean function combinations at P and Q device output ports. Some of the combinations with excellent

TABLE I Examples of Extinction Ratios for Programmable Boolean Functions

Case	$f_{\mathrm{out,P}}$		$f_{\mathrm{out,Q}}$		$\mathrm{ER_{total}}$ (dB)	$\mathrm{ER_P}$ (dB)	$\mathrm{ER_Q}$ (dB)
1	NOT A	$\overline{P_A}$	OR	$P_A + P_B$	11.3661	11.3661	11.4497
2	NOT A	$\overline{P_A}$	NOT B	$\overline{P_B}$	11.3104	11.3104	11.3104
3	NOT B	$\overline{P_B}$	NOT A	$\overline{P_A}$	11.3104	11.3105	11.3104
4	OR	$P_A + P_B$	NOT A	$\overline{P_A}$	11.2638	11.3736	11.7578
5	OR	$P_A + P_B$	NOT B	$\overline{P_B}$	10.9270	11.0806	11.6232
6	NOT B	$\overline{P_B}$	OR	$P_A + P_B$	10.6350	10.6350	11.4948
7	NOT B	$\overline{P_B}$	XOR	$P_A \oplus P_B$	7.8674	10.1202	7.8674
8	NOT A	$\overline{P_A}$	XOR	$P_A \oplus P_B$	7.7665	10.5350	7.7665
9	OR	$P_A + P_B$	NOR	$\overline{P_A + P_B}$	7.5821	13.4070	7.5821
10	XOR	$P_A \oplus P_B$	NOT A	$\overline{P_A}$	7.4774	7.4774	10.9892
11	XOR	$P_A \oplus P_B$	NOT B	$\overline{P_B}$	7.3192	7.3192	11.1307
12	NOR	$\overline{P_A + P_B}$	OR	$P_A + P_B$	7.0385	7.0385	9.3537
13	NOR	$\overline{P_A + P_B}$	XOR	$P_A \oplus P_B$	6.3011	6.5146	7.0522
14	XOR	$P_A \oplus P_B$	NOR	$\overline{P_A + P_B}$	6.1854	7.8396	6.5490
15	OR	$P_A + P_B$	OR	$P_A + P_B$	6.1600	7.4252	6.6100
16	NOT A	$\overline{P_A}$	NOT A	$\overline{P_A}$	5.4845	5.5473	5.5275

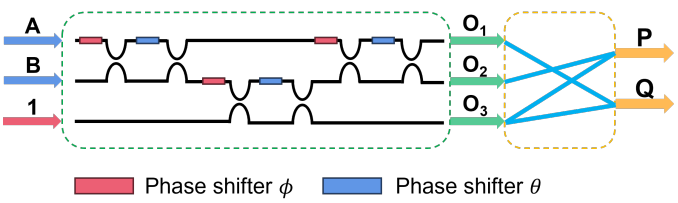

Fig. 5. Scheme of the proposed case study, namely Coupling Layer Topology number 16.

$\mathrm{ER_{total}}$ performance are listed in Table I. The second to fifth columns of the table specify the expressions of the Boolean functions in each port. The sixth column reports the $\mathrm{ER_{total}}$ as defined in Eq. (4) to quantify the overall performance of the case study; Table I is sorted in descending order according to the value of $\mathrm{ER_{total}}$ reported in this column. The last two columns of the table exhibit the signal quality in each port respectively, which is calculated as:

$$\mathrm{ER}_k(\mathrm{dB}) = 10\log_{10}\left(\frac{\min(P_{1,k})}{\max(P_{0,k})}\right) \tag{10}$$

where $\mathrm{ER}_k(\mathrm{dB})$ is the extinction ratio for the power measured at the k-th port. $P_{1,k}$ represents the power value of logical "1" cases at the k-th port. $P_{0,k}$ represents the power value of logical "0" cases at the k-th port (k refers to P and Q output ports, respectively).

As shown in Table I, the case study can support at least 16 Boolean functions with an $\mathrm{ER_{total}}$ greater than 5 dB. For each case, the $\mathrm{ER_{total}}$ value is less than or at most equal to the ER_k values in each single port.

V. Conclusions and Outlook

We proposed a programmable photonic circuit scheme by attaching a practical CL topology to the 3×3 Clements mesh composed of MZI. By adopting a GA-based optimization method, we obtained the optimal phase shift values to implement every possible logical operation in each CL topology with minimal MSE. We investigated the impact of the CL topology on the ER and $\mathrm{SR}_{\%}$ values of the proposed scheme, finding that some CL topologies can reproduce more than 80% of the truth tables with an ER greater than 3 dB. We chose one of them as a case study, then looked into its capability to implement user-defined Boolean functions, determining 16 Boolean functions with an ER greater than 5 dB.

These results demonstrate the potential of this class of structures as programmable photonic circuits capable of implementing arbitrary logical operations with satisfactory output signal transmission quality, only if the optimal phase shift values of MZI are set and the proper optical coupling topology is adopted. These principles can be applied to more complex photonic structures, which sheds light on photonic chip design and testing.

References

[1] B. J. Shastri *et al.*, "Photonics for artificial intelligence and neuromorphic computing," *Nature Photonics*, vol. 15, pp. 102–114, 2021.

[2] D. Pérez *et al.*, "Multipurpose silicon photonics signal processor core," *Nature Communications*, vol. 8, p. 636, 2017.

[3] J. Xu *et al.*, "Progress in silicon-based reconfigurable and programmable all-optical signal processing chips," *Frontiers of Optoelectronics*, vol. 18, p. 10, 2025.

[4] H. Chen, H. Chen, and E. H. Chan, "Simple and reconfigurable all-optical logic gate," *Optics & Laser Technology*, vol. 170, p. 110297, 2024.

[5] X. Gao *et al.*, "Seven-channel all-optical reconfigurable canonical logic units multicasting at 40 Gb/s based on a nonlinearity-enhanced silicon waveguide," *Optics Express*, vol. 30, pp. 32650–32659, 2022.

[6] Y. Shen *et al.*, "Deep learning with coherent nanophotonic circuits," *Nature Photonics*, vol. 11, pp. 441–446, 2017.

[7] J. Chen *et al.*, "Optical logic operations using a meshed Mach-Zehnder interference array," *Optics & Laser Technology*, vol. 167, p. 109703, 2023.

[8] A. Marchisio, F. D. Ros, V. Curri, A. Carena, and P. Bardella, "Comprehensive model of MZI-based circuits for photonic computing applications," *Communications Physics*, vol. 8, p. 277, 2025.

[9] W. R. Clements, P. C. Humphreys, B. J. Metcalf, W. S. Kolthammer, and I. A. Walmsley, "Optimal design for universal multiport interferometers," *Optica*, vol. 3, no. 12, pp. 1460–1465, 2016.

[10] S. Forrest, "Genetic Algorithms: Principles of Natural Selection Applied to Computation," *Science*, vol. 261, no. 5123, pp. 872–878, 1993.